

# Genetic Analysis of the Hox Hydrogenase in the Cyanobacterium *Synechocystis* sp. PCC 6803 Reveals Subunit Roles in Association, Assembly, Maturation, and Function<sup>\*[5]</sup>

Received for publication, June 15, 2012, and in revised form, November 7, 2012. Published, JBC Papers in Press, November 8, 2012, DOI 10.1074/jbc.M112.392407

Carrie Eckert<sup>†1</sup>, Marko Boehm<sup>‡§</sup>, Damian Carrieri<sup>‡</sup>, Jianping Yu<sup>‡</sup>, Alexandra Dubini<sup>‡</sup>, Peter J. Nixon<sup>§</sup>, and Pin-Ching Maness<sup>‡</sup>

From the <sup>‡</sup>Biosciences Center, National Renewable Energy Laboratory, Golden, Colorado 80401 and the <sup>§</sup>Department of Life Sciences, Imperial College London, South Kensington Campus, London SW7 2AZ, United Kingdom

**Background:** Hox hydrogenase (HoxEFUYH) is present in some bacteria and cyanobacteria.

**Results:** In *Synechocystis*, HoxYH and HoxEFU form subcomplexes that can be disrupted in Hox subunit mutants.

**Conclusion:** Hox assembly is modular and most reliant on the presence of HoxF and -U, consistent with effects on Hox protein abundance and activity.

**Significance:** Subcomplexes of Hox hydrogenase may represent steps in complex assembly and maturation.

Hydrogenases are metalloenzymes that catalyze  $2\text{H}^+ + 2\text{e}^- \leftrightarrow \text{H}_2$ . A multisubunit, bidirectional [NiFe]-hydrogenase has been identified and characterized in a number of bacteria, including cyanobacteria, where it is hypothesized to function as an electron valve, balancing reductant in the cell. In cyanobacteria, this Hox hydrogenase consists of five proteins in two functional moieties: a hydrogenase moiety (HoxYH) with homology to heterodimeric [NiFe]-hydrogenases and a diaphorase moiety (HoxEFU) with homology to NuoEFG of respiratory Complex I, linking  $\text{NAD(P)H} \leftrightarrow \text{NAD(P)}^+$  as a source/sink for electrons. Here, we present an extensive study of Hox hydrogenase in the cyanobacterium *Synechocystis* sp. PCC 6803. We identify the presence of HoxEFUYH, HoxFUYH, HoxEFU, HoxFU, and HoxYH subcomplexes as well as association of the immature, unprocessed large subunit (HoxH) with other Hox subunits and unidentified factors, providing a basis for understanding Hox maturation and assembly. The analysis of mutants containing individual and combined *hox* gene deletions in a common parental strain reveals apparent alterations in subunit abundance and highlights an essential role for HoxF and HoxU in complex/subcomplex association. In addition, analysis of individual and combined *hox* mutant phenotypes in a single strain background provides a clear view of the function of each subunit in hydrogenase activity and presents evidence that its physiological function is more complicated than previously reported, with no outward defects apparent in growth or photosynthesis under various growth conditions.

Hydrogenase enzymes are a unique and diverse family of metalloenzymes widely distributed throughout Archaea, Prokaryotes, and some unicellular Eukaryotes that catalyze the reduction/oxidation of  $\text{H}^+/\text{H}_2$ . These enzymes are classified by their metal-containing active sites and include [Fe]-hydrogenases, [FeFe]-hydrogenases, and [NiFe]-hydrogenases (1). The [NiFe]-hydrogenases are minimally heterodimeric, consisting of a large catalytic subunit and a small subunit containing at least one [FeS] cluster that functions in electron transfer to and from the large subunit (1). The maturation of [NiFe]-hydrogenases involves at least six maturation proteins (HypABCDEF) essential for the assembly of the [NiFe] active site. Some [NiFe]-hydrogenases additionally require a specialized protease that cleaves the large subunit's C terminus, a step required for hydrogenase function (2). Research in *Escherichia coli* suggests that the hydrogenase small subunit only associates with the large subunit after it is fully processed (3).

Among the diverse hydrogenases, the bidirectional [NiFe]-hydrogenase (Hox) in cyanobacteria is of great interest for basic biological study as well as for the development of solar hydrogen production technologies (4–6). NAD(P)-linked Hox hydrogenases have been identified and characterized in cyanobacteria (4, 5), the Gram-positive bacterium *Rhodococcus opacus* (7, 8), the Gram-negative bacterium *Ralstonia eutropha* (6), and the purple sulfur photosynthetic bacteria *Thiocapsa roseopersicina* and *Allochrochromatium vinosum* (9–12). These Hox hydrogenases are multimeric with at least four related subunits expressed from a single operon. HoxH and HoxY form the hydrogenase moiety and are homologous to the large and small subunits of prototypical heterodimeric [NiFe]-hydrogenases, respectively (1). The [FeS] cluster-containing subunits HoxF, HoxU, and, in some organisms, HoxE form the diaphorase moiety (13, 14) that catalyzes the oxidation/reduction of  $\text{NAD(P)H}/\text{NAD(P)}^+$  (via FMN and NAD binding sites in HoxF) coupled to the hydrogenase moiety (HoxYH) (10, 12–15). The *R. eutropha* Hox hydrogenase does not contain HoxE and instead harbors an unrelated fifth subunit, HoxI, which functions in linkage to NADPH (16).

\* This work was supported by the National Renewable Energy Laboratory's Laboratory Directed Research and Development Program (to P. M., J. Y., C. E., and D. C.), the United States Department of Energy Fuel Cell Technologies Program (contract number DE-AC36-08-GO28308) (to P. M. and J. Y.), the United States Department of Energy Biological and Environmental Research Program (contract KP160103) (to M. B. and A. D.), and Engineering and Physical Sciences Research Council Grant (EP/F002070X/1) (to M. B. and P. N.).

[5] This article contains supplemental Table 1 and Figs. 1–5.

<sup>†</sup> To whom correspondence should be addressed: Biosciences Center, NREL, 15013 Denver West Pkwy., Golden, CO 80401. Tel.: 303-384-6891; Fax: 303-384-7836; E-mail: carrie.eckert@nrel.gov.

## EXPERIMENTAL PROCEDURES

Purification of the Hox hydrogenase has been performed in some of the organisms it has been characterized in with varied results. In *R. eutropha*, the purified Hox complex is HoxFU<sub>2</sub>YH<sub>2</sub>, although HoxI (not present in other characterized Hox hydrogenases) dissociates easily upon more stringent purification conditions (which is why the complex was initially characterized as HoxFU<sub>2</sub>YH) (16). Other purifications in *R. eutropha* utilizing gene knockouts and ectopic expression demonstrate that HoxYH and HoxFU subcomplexes can be isolated, although these subcomplexes were reportedly unstable (13). In *A. vinosum* (12) and the cyanobacterium *Gleocapsa alpicola* CALU 743 (17), attempted purifications of native complex resulted in isolation of only HoxYH, whereas in *T. roseopersicina* (18) and *Synechocystis* (19, 20), intact HoxEFU<sub>2</sub>YH complexes were purified. Purification of the *Synechocystis* Hox hydrogenase by Schmitz *et al.* (19) resulted in a dimer of a 1:1:1:1:1 HoxE/F/U/Y/H complex via a series of column chromatography steps, whereas Germer *et al.* (20) purified a complex with a 0.2:2:2:1:1 HoxE/F/U/Y/H ratio using a StrepII-tagged HoxF, raising questions about Hox complex assembly and association *in vivo*.

The physiological role of Hox hydrogenase varies, depending on the organism in which it is present, but it generally functions in anoxic/micro-oxic conditions due to a reversible inactivation by O<sub>2</sub> (1). In *T. roseopersicina*, Hox hydrogenase catalyzes H<sub>2</sub> production under dark, fermentative conditions and in light when thiosulfate is present and alternatively functions in H<sub>2</sub> uptake in light when O<sub>2</sub> is absent (11). The Hox hydrogenase of *R. eutropha* (soluble hydrogenase) functions in H<sub>2</sub> oxidation linked to the regeneration of NADH in support of carbon fixation (6). In cyanobacteria, Hox hydrogenase is expressed under both anaerobic and aerobic conditions (4, 21) but is only active under dark, fermentative conditions and in the transition from dark to light prior to inhibition by O<sub>2</sub> generated during photosynthesis (22–24). Respiration and nitrate assimilation mutants exhibit increased H<sub>2</sub> photoevolution rates under low O<sub>2</sub> conditions, whereas defects in photosynthetic reactions/ratios have been reported in Hox hydrogenase mutants (15, 22–26). Therefore, it is hypothesized that the Hox hydrogenase functions as an electron valve for cells by H<sub>2</sub> production/oxidation in response to changes in redox states (25, 26). HoxEFU are the only homologs for NuoEFG of respiratory complex I in cyanobacteria, but there is no evidence to date that these diaphorase subunits play any role in respiration (14, 27–30).

In this work, we generated a series of Hox hydrogenase mutants in a common parental strain, deleting individual *hox* genes or combinations of *hox* genes in the unicellular cyanobacterium *Synechocystis* sp. PCC 6803. This comprehensive collection of *hox* mutants enabled us to perform systematic studies of mutation effects on complex/subcomplex formation and composition, subunit abundance, and hydrogenase activity. In addition, we also provide data for growth, photosynthesis, and fermentation in a *hox* operon deletion mutant compared with wild type (WT), revealing that some previously reported *hox* mutant phenotypes may have been due to differences in strain backgrounds (31, 32).

**Strain Background/Construction**—All *hox* mutants were generated in a *Synechocystis* sp. PCC 6803 glucose-tolerant strain from Teruo Ogawa, who also provided the whole operon deletion, *hox*<sup>−</sup>::hygromycin resistance. The *hoxH*<sup>−</sup> deletion was constructed in a pSMART LC-Amp vector (Lucigen, Inc.) containing a 3.6-kb region spanning *hoxY* and *hoxH* cut with SspI (removing 816 bp of *hoxH*) to insert the kanamycin resistance cassette from pUC4K. All remaining *hox* deletion strains were created by two-step fusion PCR (33) for open reading frame (ORF) replacement, combining ~600-bp 5′- and 3′-flanking regions for each *hox* gene ORF replaced with the following antibiotic resistance gene ORFs: *hoxE*<sup>−</sup>::*aac3ia* (gentamicin resistance), *hoxF*<sup>−</sup>::*ermC* (erythromycin resistance), *hoxU*<sup>−</sup>::*aph* (kanamycin resistance), and *hoxY*<sup>−</sup>::*dfra17* (spectinomycin resistance). An *slr0168* neutral site integration vector containing a plastocyanin (*petE*) promoter for ectopic gene expression (34) was altered by the addition of a 225-bp fragment from pETDuet containing the T7 terminator into the PpuMI restriction site. PCR primers to amplify HoxYH or HoxH from genomic DNA were constructed with sequence encoding His<sub>6</sub>/HRV3C protease site at the N terminus and 5′- and 3′-specific SapI sites for insertion behind the *petE* promoter following restriction digestion and ligation. The pPSBA2KS vector for the integration behind the *psbAII* promoter (35) was altered by removal of a Sall site via partial digest and blunting to allow for retention of the kanamycin resistance gene. PCR primers were designed for amplification and insertion of an N-terminal His<sub>6</sub>-tagged *hoxE* gene between NdeI and Sall sites. Transformations were conducted by incubating ~1 μg of linear purified fusion PCR products or targeted integration vectors with 200 μl of cells (adjusted to OD<sub>730</sub> = 2.5 from cell cultures at OD<sub>730</sub> = 0.2–0.5) for 6 h, followed by the addition of 2 ml of BG11, 24-h outgrowth in culture tubes under standard growth conditions, and plating of 200 μl on BG11 plates with antibiotics as required for selection (200 μg/ml hygromycin or kanamycin, 100 μg/ml gentamicin, erythromycin, spectinomycin, or chloramphenicol).

**Strain Growth**—Cultures were inoculated into BG11 medium (ATCC medium 616) supplemented with 3 μM NiCl<sub>2</sub>, 20 mM TES (unbuffered), 100 mM NaHCO<sub>3</sub>, and antibiotics as required (one-half concentrations as used on plates listed above) at an initial OD<sub>730</sub> = 0.05 and were grown by shaking in culture flasks with 5% CO<sub>2</sub> under 50 microeinsteins<sup>2</sup> (μE) m<sup>−2</sup> s<sup>−1</sup> continuous light from cool white fluorescent bulbs. Cultures were generally grown to logarithmic/linear growth phase (OD<sub>730</sub> = 0.2–0.8) for analysis.

**FPLC Analysis of *Synechocystis* sp. PCC 6803 WT Soluble Extract**—Soluble extract was prepared from a WT 50-ml liquid culture at an OD<sub>730</sub> > 1 (stationary phase). Cells were harvested, resuspended, and washed twice in ACA buffer (750 mM ε-amino caproic acid, 50 mM BisTris/HCl, pH 7.0, 0.5 mM EDTA). Approximately 200 μl of glass beads (150–212 μm;

<sup>2</sup>The abbreviations used are: μE, microeinsteins; MV, methyl viologen; BN, blue native; PSI and PSII, photosystem I and II, respectively; ETR, electron transport rate; BisTris, 2-[bis(2-hydroxyethyl)amino]-2-(hydroxymethyl)propane-1,3-diol.

## Cyanobacterial Hox Hydrogenase Complex Association and Function

Sigma-Aldrich) were added to the cell suspension ( $\sim 500 \mu\text{l}$ ), and cells were broken using a Disruptor Genie digital multi-place vortexer (Scientific Industries) at  $4^\circ\text{C}$  for 5 min, setting 3,000, followed by centrifugation for 10 min at maximum speed in a microcentrifuge. Subsequently,  $2 \mu\text{l}$  of DNase I (10,000 units/ml, Thermo Scientific) was added, and the sample was spun again in an ultracentrifuge at  $100,000 \times g$  for 30 min at  $4^\circ\text{C}$ . For FPLC, the resulting supernatant was normalized to  $\text{OD}_{650} = 10$  (typically, the  $\text{OD}_{650}$  of a 1:20 dilution was measured). To solubilize any remaining thylakoid membrane fragments,  $\beta$ -dodecyl-D-maltoside was added to a final concentration of 0.5% (w/v) from a 10% (w/v) stock solution.  $100 \mu\text{l}$  of this soluble extract was loaded onto a Superdex 200 10/300 size exclusion column (GE Healthcare) connected to an Akta Purifier FPLC system (GE Healthcare). The sample was run at a flow rate of  $0.5 \text{ ml min}^{-1}$  with 50 mM Tris, pH 7.5, 100 mM NaCl, and 0.03% (w/v)  $\beta$ -dodecyl-D-maltoside as the buffer. 0.5-ml fractions were collected by a Frac-950 fraction collector (GE Healthcare). A high molecular weight marker mix (GE Healthcare) was run as a control for relative protein sizes in the fractions (supplemental Fig. 1).

**Protein Preparations, Two-dimensional Blue Native/SDS-PAGE, Affinity Purification, and Western Blotting**—Soluble extracts for two-dimensional blue native/SDS-PAGE (BN/SDS-PAGE) were prepared as described for FPLC analysis above for WT and *hox* mutant strains, and the extracts were normalized to an  $A_{650} = 0.6$ .  $\beta$ -Dodecyl-D-maltoside was added to a final concentration of 0.5% (w/v), and the same volume of Coomassie loading solution (750 mM  $\epsilon$ -amino caproic acid, 5% (w/v) Coomassie-G) was added to the sample. Subsequently,  $20 \mu\text{l}$  of the sample was loaded per lane and run on a 12% (w/v) polyacrylamide BN PAGE first dimension gel. The protein complexes in the first dimension gel strips were denatured for 1 h in solubilization buffer (66 mM  $\text{Na}_2\text{CO}_3$ , 2% (w/v) SDS, 2% (v/v)  $\beta$ -mercaptoethanol, and 4 M urea) prior to being layered on 17.5% (w/v) polyacrylamide, 6 M urea two-dimensional SDS-polyacrylamide gels (36). The resultant two-dimensional gels were either Coomassie-stained, silver-stained (37), or electroblotted onto nitrocellulose membranes.

For WT and *hox* mutant one-dimensional Western blots and affinity purifications, cells were resuspended in 20 mM phosphate buffer, pH 7.4, plus protease inhibitors (Fermentas) and broken by bead disruption as described above. Protein concentrations were determined by Bradford assay (Fermentas), and levels of each sample were adjusted to  $\sim 100 \mu\text{g/ml}$ . For purification of His<sub>6</sub>-tagged proteins/complexes,  $\text{Co}^{2+}$  beads (Pierce) were added to cleared lysates and incubated for 1 h at  $4^\circ\text{C}$ , and washes were performed using 5 times bead volume with 20 mM phosphate buffer, pH 7.4, with or without 0.5 M NaCl through reloadable columns (Pierce). Beads were resuspended in a 50% slurry in buffer. To rule out nonspecific binding of Hox proteins to beads, untagged WT samples were also subjected to the same regime, and a lack of Hox proteins in bead samples was verified by Western blot (data not shown). Samples for SDS-PAGE were boiled in  $1\times$  Laemmli sample buffer (Bio-Rad), and  $10 \mu\text{l}$  of each was loaded onto precast TGX Stain-free Any kDa gels (Bio-Rad) and transferred onto a PVDF membrane (Bio-Rad). For Western blotting, the SnapID system (Millipore) was used

according to the manufacturer's instructions. Membranes were blocked in 5% BSA,  $1\times$  PBST, and primary and secondary antibodies were diluted in 1% BSA,  $1\times$  PBST. Polyclonal rabbit primary antibodies developed for this study were generated using  $\sim 20$ -amino acid C-terminal peptides ( $\alpha$ -HoxE, -F, -U, -Y, and -H (C-terminal);  $\alpha$ -HoxF and  $\alpha$ -HoxY from these preparations are not shown but were used in quantitation of one-dimensional Western blots) and a HoxH internal peptide (amino acids 300–318) that allows recognition of both processed and unprocessed HoxH (YenZym, San Francisco, CA).  $\alpha$ -HoxY and  $\alpha$ -HoxF antibodies were also generated in rabbit using full-length *E. coli* expressed protein (SeqLab).  $\alpha$ -Rps1 (Agriseria; not shown) and  $\alpha$ -PsaD antibodies (38) were used as loading controls for normalization of band intensities for relative protein level quantitation. Secondary incubation was performed with Clean Blot HRP (Pierce), and Cell Biosciences ChemiWest or Pierce Dura Chemiluminescent reagents were used for signal development. Images and quantitation analysis were processed using a Cell Biosciences FluoroCam Q Gel imaging system.

**Hydrogenase Assays**—Cells grown to similar logarithmic growth densities ( $\text{OD}_{730} = 0.2\text{--}0.8$ ) were concentrated to  $\text{OD}_{730} = 2.5$ , and  $200 \mu\text{l}$  was added to  $600 \mu\text{l}$  of assay mixture containing Triton X-100 (0.05%, w/v), phosphate buffer (50 mM, pH 7), and either methyl viologen (MV; 1 mM final) or NADH (1 mM final) in 2-ml HPLC vials sealed with anaerobic septa. The mixture was sparged with argon for 10 min,  $100 \mu\text{l}$  of anaerobic sodium dithionite (10 mM final) was added, and the mixture was incubated with shaking for 30 min at  $37^\circ\text{C}$ . The reaction was stopped by the addition of  $100 \mu\text{l}$  of 20% (w/v) trichloroacetic acid, and  $100 \mu\text{l}$  of the 1-ml headspace was analyzed using a gas chromatograph (Agilent 1100) equipped with a Molecular Sieve 5A column, a thermal conductivity detector, and argon as the carrier gas. To measure *in vivo*  $\text{H}_2$  production, cells were spun down and resuspended to  $\text{OD}_{730} = 2.5$  in 2 ml of BG11 containing 5 mM glucose, placed in a 15-ml culture tube, sealed with anaerobic septum, sparged with argon for 30 min, and incubated at  $30^\circ\text{C}$  in the dark for 24 h. A  $100\text{-}\mu\text{l}$  sample from the 13-ml headspace was analyzed using a gas chromatograph as above.

**Determination of Doubling Times**—Log phase precultures (10 ml) of WT and *hox*<sup>−</sup> strains were used to inoculate 400-ml capacity Photobioreactor culture vessels (FMT 400, Photon System Instruments) without the addition of antibiotic to growth medium. Illumination parameters were programmed as listed in Table 1. Optical density was measured every 1–5 min at wavelength maximum 680 nm and recorded digitally, along with pH and  $\text{O}_2$  concentration (not shown). Culture vessels were maintained at  $30^\circ\text{C}$  and continuously bubbled at a rate of  $\sim 250 \text{ ml/min}$  in air or argon supplemented with 2%  $\text{CO}_2$ . Optical density values *versus* time were fitted to a single exponential function to determine doubling times.

**Fluorescence Measurements**—Dark-adapted quantum efficiency ( $F_v/F_m$ ) and effective quantum efficiency under illumination ( $\Delta F/F_m'$ ) of WT and *hox*<sup>−</sup> strain suspensions from log phase cultures were measured in multiwell plates with a closed FluorCam (FC 800-C/1010, Photon System Instruments) and used to calculate effective electron transport rates.  $\Delta F/F_m'$  was determined for cells under continuous illumination for at least

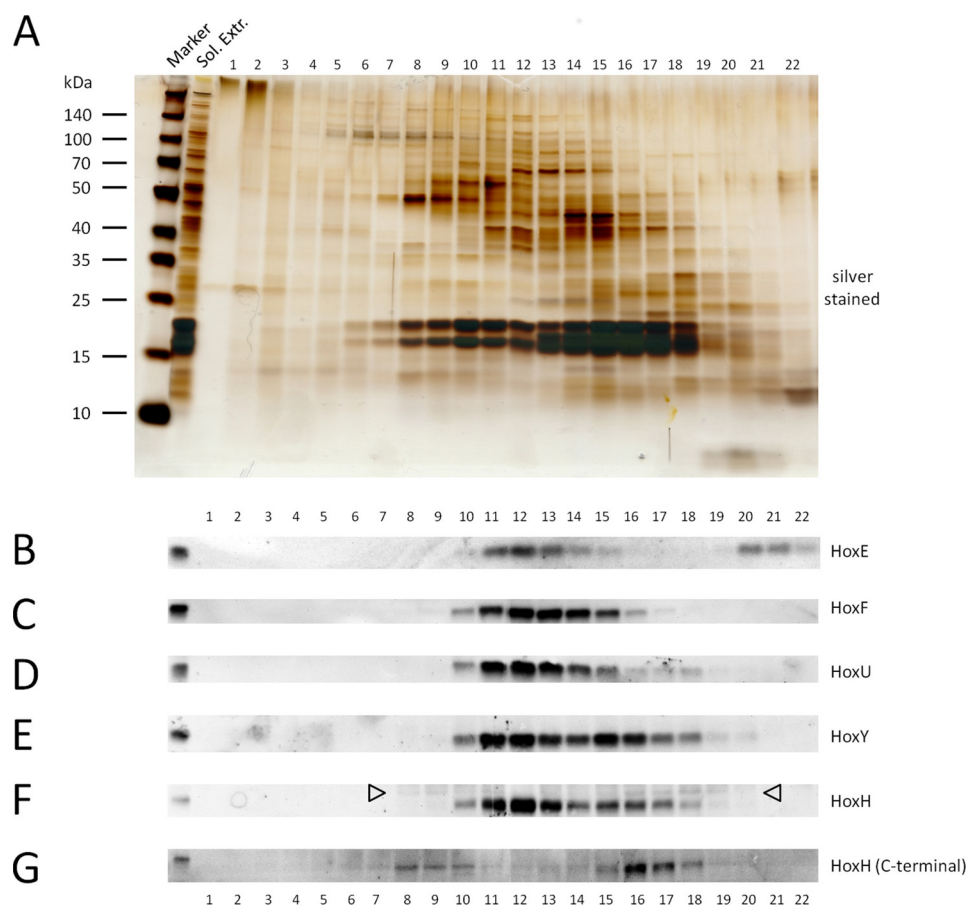


**FIGURE 1. FPLC and Western blot analysis of WT *Synechocystis* sp. PCC 6803 Hox hydrogenase.** The crude soluble fraction of WT *Synechocystis* sp. PCC 6803 was separated by FPLC, and the resulting fractions were analyzed by Western blotting. *A*, silver-stained TGX Any kDa gradient SDS-polyacrylamide gel (Bio-Rad) of starting material (*Sol. Extr.*) and fractions 1–22 (for the chromatogram at  $A_{280}$  and  $A_{420}$  see [supplemental Fig. 1](#)). *B–G*, Western blotting of FPLC fractions with the indicated Hox subunit-specific antibodies. *Arrowheads* in *F* indicate the signal for unprocessed HoxH.

3 min at each light intensity with dark adaption between experiments. Cells were dark-adapted for at least 5 min prior to measurement and were measured in biological and technical triplicate (minimum number of samples per type = 9).

## RESULTS

**Composition of Hox Hydrogenase Protein Complexes**—Reported subunit composition and stoichiometry of purified Hox hydrogenase varies in the literature (12, 16–20), raising questions about its *in vivo* structure. Therefore, we assessed fractionation of the Hox hydrogenase complex by performing size exclusion FPLC analysis of *Synechocystis* WT soluble extracts followed by Western blotting with Hox subunit-specific antibodies (Fig. 1). As expected, all five subunits, HoxE (18.8 kDa), HoxF (57.8 kDa), HoxU (26.2 kDa), HoxY (20.0 kDa), and HoxH (52.9 kDa), clearly co-fractionate (fractions 10–14). The band intensities of the diaphorase (HoxEFU) and hydrogenase (HoxYH) subunits fluctuate in a related manner, consistent with HoxYH and HoxEFU subcomplexes observed in purifications of other Hox hydrogenases (12, 16, 17). The presence of what is probably monomeric HoxE (fractions 20–22) suggests that HoxE may dissociate relatively easily from the complex. Interestingly, unprocessed, immature HoxH co-fractionates with other Hox proteins, including processed HoxH (fractions 10 and 16–18), implying association of unprocessed HoxH with

other complex subunits prior to maturation and full complex assembly (Fig. 1, HoxH (*open arrows*) and HoxH (C-terminal) blots). In addition, unprocessed HoxH is clearly present in higher molecular weight complexes (fractions 8 and 9), revealing its association with other unknown proteins (possibly maturation factors) prior to its cleavage.

Results from size exclusion FPLC imply the presence of Hox complexes and possible subcomplexes, but co-fractionation does not provide enough evidence to confirm subunit association. To verify Hox protein complex/subcomplex associations in soluble extracts, we performed two-dimensional BN/SDS-PAGE followed by Western blotting (Fig. 2). Using this approach, we were able to identify a complex containing all five Hox subunits, again consistent with the composition of the purified pentameric complex reported in the literature (19, 20). The apparent molecular mass of this complex is ~160 kDa, close to the calculated mass based on the predicted sizes of the individual subunits (175 kDa). We note that no dimer of this pentameric hydrogenase protein complex could be reliably detected in our analysis despite previous reports (19). However, we were able to detect the presence of HoxFUYH, HoxEFU, and HoxFU subcomplexes. We also failed to reliably detect a HoxYH subcomplex, yet there was a weak antibody signal for the HoxH subunit with a higher apparent molecular mass than

## Cyanobacterial Hox Hydrogenase Complex Association and Function

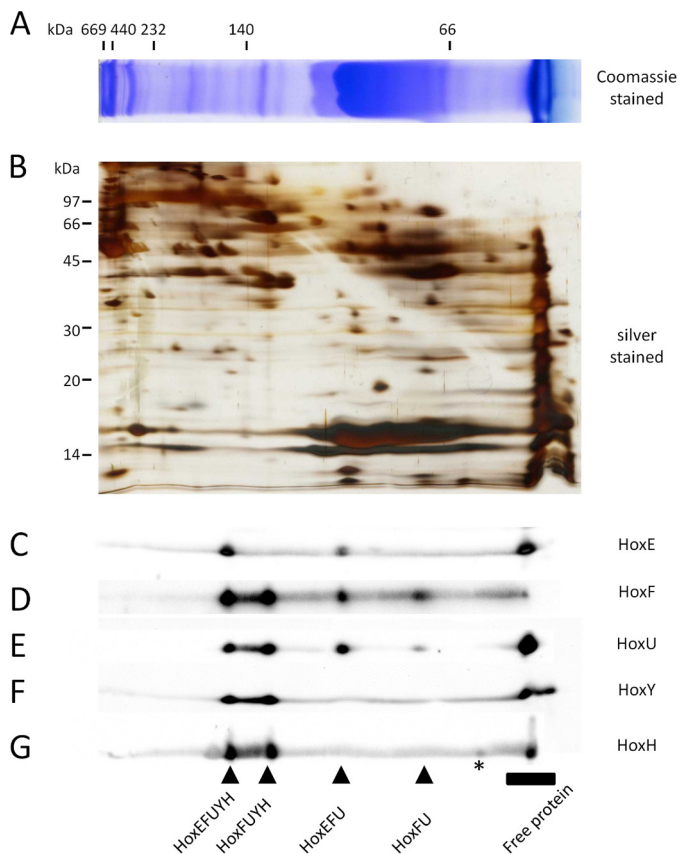


**FIGURE 2. Two-dimensional BN/SDS-PAGE and Western blot analysis of WT *Synechocystis* sp. PCC 6803 Hox hydrogenase.** A, the soluble fraction of WT *Synechocystis* sp. PCC 6803 was separated on a 12% (w/v) polyacrylamide BN-polyacrylamide gel followed by two-dimensional separation on a 17.5% (w/v) polyacrylamide SDS-polyacrylamide gel (B) and analysis by Western blotting with the indicated Hox subunit-specific antibodies (C–G). The first dimension BN-polyacrylamide gel was Coomassie-stained, whereas the second dimension SDS-polyacrylamide gel was silver-stained.

that of the free HoxH protein alone (Fig. 2G, asterisk), suggesting the association of HoxH with another protein. Monomeric subunits were also detected in the low molecular mass region of the Western blots, with the HoxE, HoxH, and HoxU subunits all accumulating to significant levels when compared with levels of each associated with subcomplexes. We were unable to consistently detect unprocessed HoxH in any of these subcomplexes, suggesting that its possible association may only be transient. Nevertheless, these data reveal for the first time the presence of various subcomplexes of *Synechocystis* Hox hydrogenase *in vivo*.

**Subunit Abundance in Hox Hydrogenase Mutants**—The detection of Hox subcomplexes in the WT strain by FPLC and two-dimensional BN/SDS-PAGE analyses prompted us to construct mutants of each *hox* gene alone and in combination in the same parental WT strain (supplemental Fig. 2) to further examine any relationship between complex/subcomplex associations and relative subunit abundance by Western blotting. All of the mutants except for *hox*<sup>−</sup> (whole operon deletion constructed by T. Ogawa) and *hoxH*<sup>−</sup> (see “Experimental Procedures” and supplemental Fig. 2) were created by ORF replacement with similar size antibiotic resistance genes to avoid changes in operon transcription from additional promoters in antibiotic resistance cassettes or large alterations in sequence

size. As expected, no detectable Western signal for Hox subunits was apparent when the respective gene was disrupted, confirming full segregation of gene deletions (cyanobacteria carry multiple genome copies) (Fig. 3A). Interestingly, deletion of *hoxE*, the first gene in the operon, led to a 2–3-fold increase in the remaining Hox protein subunits (Fig. 3B). The increase in Hox protein levels in this mutant is probably linked to the first 190 bp of the *hoxE* ORF, whose absence results in increased *hox* transcript levels and possible enhancement in the rate of translation due to a decrease in minimum free energy in the *hoxE*<sup>−</sup> mutant mRNA (see “Discussion” and supplemental Fig. 3, A–D). The overexpression of HoxH in the *hoxE*<sup>−</sup> mutant leads to a discernible increase in levels of unprocessed HoxH compared with WT and other *hox* mutants (Fig. 3A and supplemental Fig. 4), consistent with increased unprocessed large subunit when the hydrogenase is overexpressed without additional maturation factors in previous studies (our unpublished results<sup>3</sup> for *R. eutropha* soluble hydrogenase and Refs. 13 and 20). All other *hox* mutants exhibited decreased levels of remaining complex subunits (Fig. 3B). Levels of HoxH and HoxY are decreased to 20 and 10% of WT in the respective *hoxY*<sup>−</sup> and *hoxH*<sup>−</sup> mutants, whereas HoxE, HoxF, and HoxU levels are less than 5% of WT in *hoxF*<sup>−</sup> and *hoxU*<sup>−</sup> mutants, highlighting interdependencies for HoxYH and HoxEFU subcomplex protein abundance. In addition, HoxY and HoxH levels are decreased to 15–90% of WT in HoxEFU subcomplex mutants (most notably in *hoxU*<sup>−</sup> mutants), and HoxE, HoxF, and HoxU levels are decreased to 25–70% of WT in HoxYH subcomplex mutants, revealing interdependencies in subunit abundance across subcomplexes as well.

**Hox Subunit Association in Individual Subunit *hox* Mutants**—Although changes in transcription could be responsible for altered subunit abundance observed in *hox* mutants, the absence of complex subunits could also lead to instability of the remaining subunits because of an inability to form stable Hox complexes/subcomplexes. To assess the association of the remaining Hox subunits when one of the five subunits is absent, we again performed two-dimensional BN/SDS-PAGE and Western blotting of soluble extracts from single-subunit *hox* mutants (Fig. 4). No notable differences in total protein were observed between the WT and *hox* mutant strains by Coomassie-stained one-dimensional BN or silver-stained two-dimensional SDS-polyacrylamide gels (data not shown). In the *hoxE*<sup>−</sup> strain, HoxFUYYH and HoxFU subcomplexes accumulated (Fig. 4A), consistent with the observation of those subcomplexes in WT (Fig. 2). Despite the increased levels of HoxY and HoxH in our *hoxE*<sup>−</sup> strain (Fig. 3A), we still were not able to observe the expected HoxYH subcomplex (Fig. 4A). Interestingly, none of the Hox subcomplexes are detected in *hoxF*<sup>−</sup> or *hoxU*<sup>−</sup> strains, with the remaining Hox proteins observed only as unassembled monomers, indicating that HoxF and HoxU are necessary for stable assembly/maintenance of the full Hox complex and Hox subcomplexes (Fig. 4, B and C). In contrast, the diaphorase subunits are still able to assemble into HoxEFU and HoxFU subcomplexes in *hoxY*<sup>−</sup> or *hoxH*<sup>−</sup> strains (Fig. 4, D and E), con-

<sup>3</sup> C. Eckert, J. Yu, and P.-C. Maness, unpublished results.

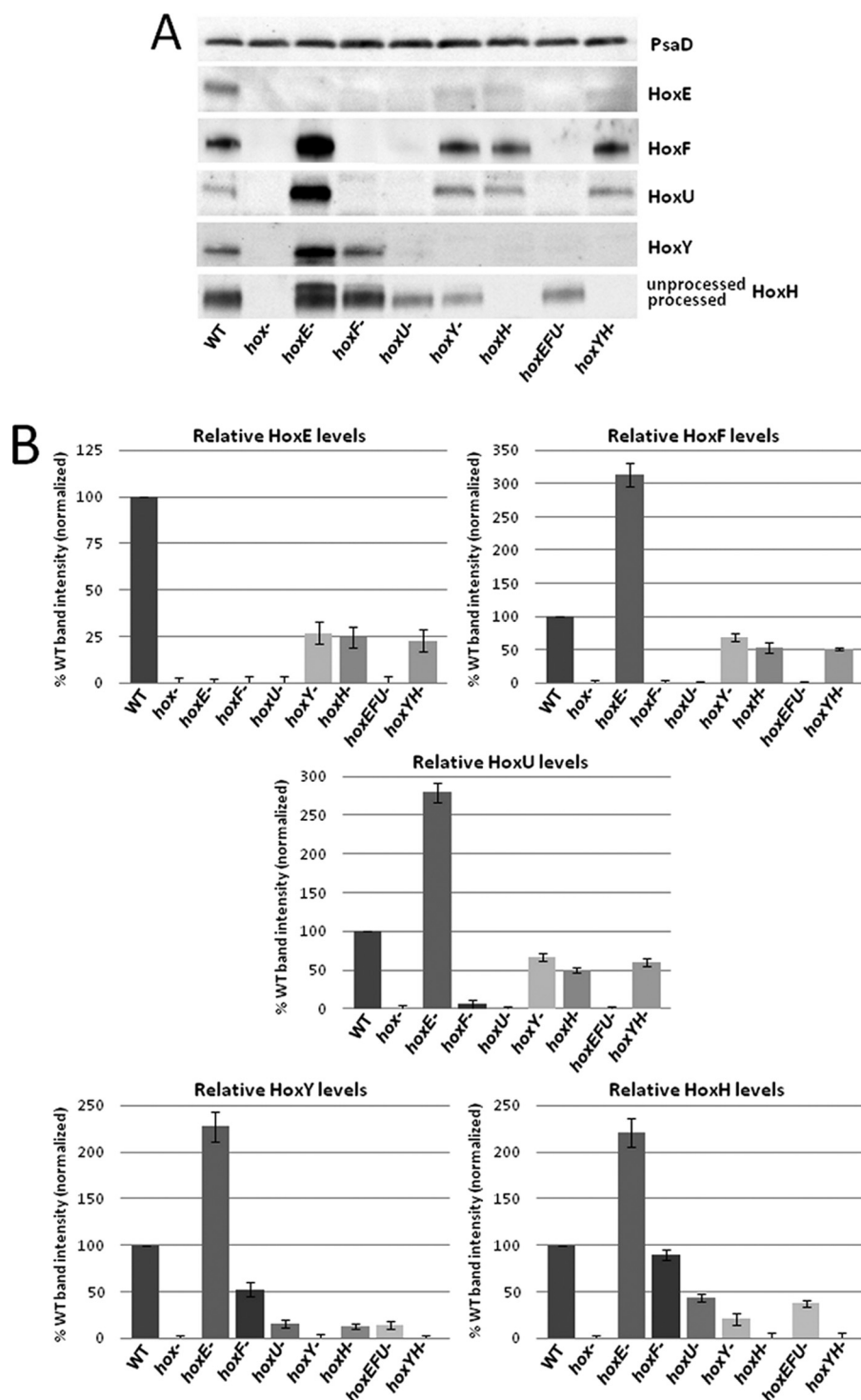


FIGURE 3. **One-dimensional SDS-PAGE and Western blot analysis of *Synechocystis* sp. PCC 6803 *hox* mutants.** *A*, whole cell lysates of WT and individual/combined *hox* mutants were run on TGX Any kDa gradient SDS-polyacrylamide gels (Bio-Rad), transferred to PVDF, and immunoblotted with Hox subunit-specific antibodies and PsaD and/or Rps1 (not shown) as loading controls. *B*, relative levels of Hox subunits in each mutant, presented as a percentage of WT. Data represent quantitation of multiple Western blot analyses with *error bars* depicting variation between separate analyses.

firming that HoxY and HoxH are not required for the stable association of diaphorase subcomplexes.

**Pull-down Analysis of Hox Subunit Associations in Hox Hydrogenase Subcomplexes**—Additional mutant strains were constructed to ectopically express His<sub>6</sub>-tagged Hox subunits to further probe subcomplex associations: 1) HoxYH, tagged on HoxY (*hox<sup>-</sup>* + His<sub>6</sub>-HoxYH); 2) HoxEFUYH, tagged on HoxH

(*hoxH<sup>-</sup>* + His<sub>6</sub>-HoxH); and 3) HoxEFUYH, tagged on HoxE (*hoxE<sup>-</sup>* + His<sub>6</sub>-HoxE). Overexpression of HoxH by ectopic expression (Fig. 5, *A* and *B*) or in the *hoxE<sup>-</sup>* strain background (Fig. 5C) results in clear unprocessed and processed HoxH signal (Fig. 5, *A–C*, *upper* and *lower* bands, respectively, in HoxH blots and in the HoxH (C-terminal) blot), increasing the likelihood that we would see unprocessed HoxH in bead fractions if

## Cyanobacterial Hox Hydrogenase Complex Association and Function

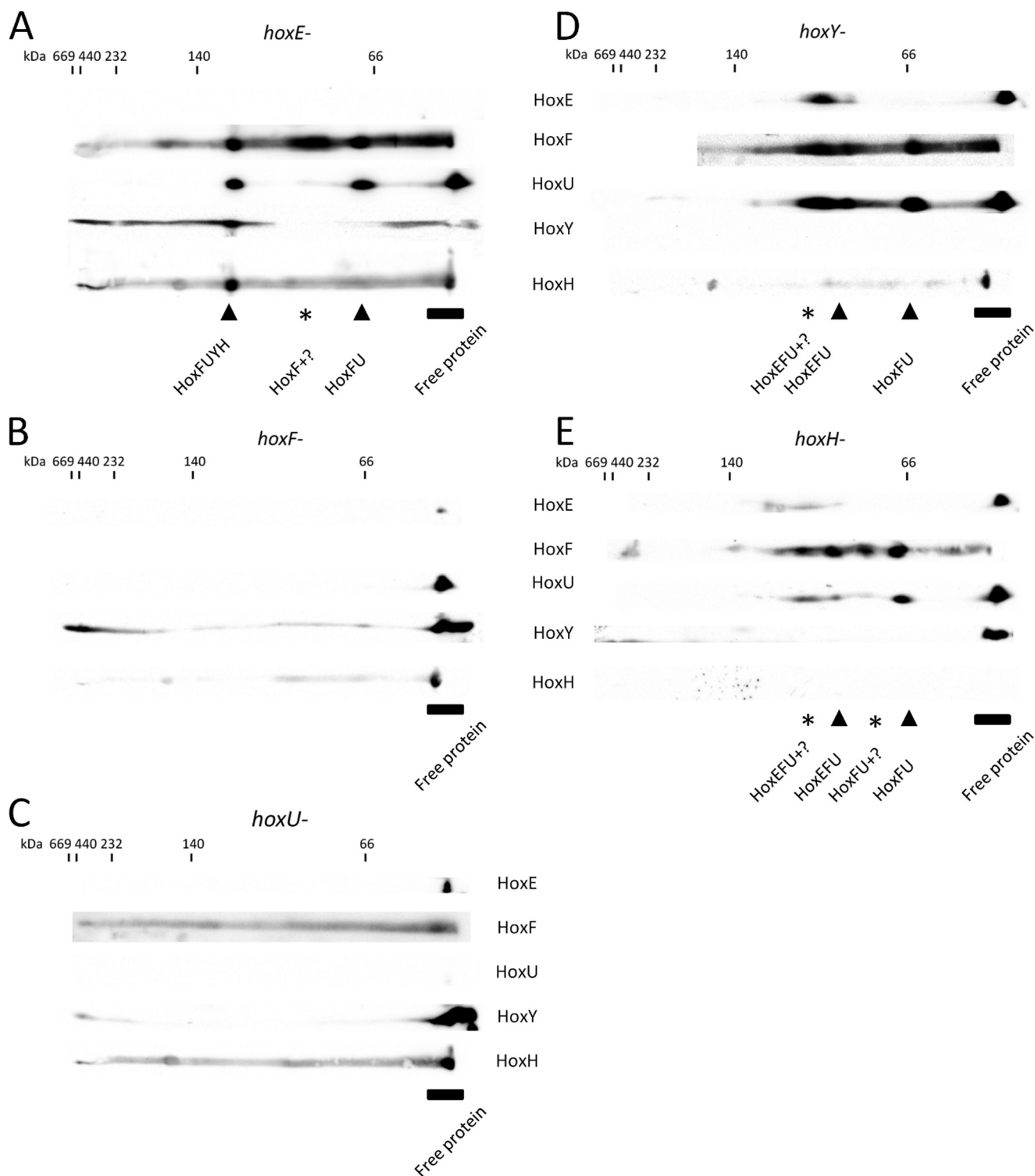


FIGURE 4. **Two-dimensional-BN/SDS-PAGE and Western blot analysis of *Synechocystis* sp. PCC 6803 *hox* mutants.** Shown are two-dimensional immunoblots (as described in the legend to Fig. 2) for *hoxE*<sup>-</sup> (A), *hoxF*<sup>-</sup> (B), *hoxU*<sup>-</sup> (C), *hoxY*<sup>-</sup> (D), and *hoxH*<sup>-</sup> (E) deletion mutant strains probed with the indicated Hox subunit-specific antibodies.

it can indeed bind complex subunits, as suggested in our FPLC analysis (Fig. 1, *F* and *G*). After ensuring that the metal-containing active site of HoxH could not bind to Co<sup>2+</sup> beads nonspecifically (data not shown; see "Experimental Procedures"), we performed pull-down assays of soluble lysates from each of these strains to verify subunit association on beads following

washes with and without 0.5 M NaCl (Fig. 5). When His<sub>6</sub>-HoxY and HoxH are co-expressed, HoxH remains bound to HoxY under all conditions, as shown by Western blotting of the bead fraction (Fig. 5A), confirming their ability to form a tightly associated HoxYH subcomplex. When a His<sub>6</sub>-tagged HoxH is used to pull down the Hox complex, only HoxY and HoxH are

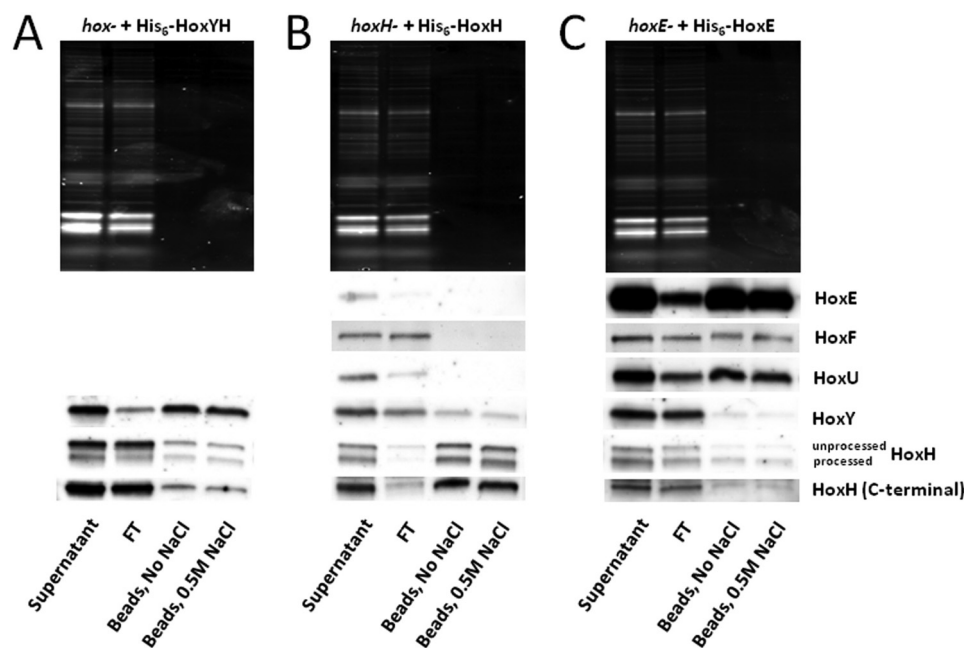


FIGURE 5. **His<sub>6</sub> pull-down of *Synechocystis* sp. PCC 6803 Hox subcomplexes.** *hox<sup>-</sup>* mutant expressing His<sub>6</sub>-HoxYH (A), *hoxH<sup>-</sup>* mutant expressing His<sub>6</sub>-HoxH (B), and *hoxE<sup>-</sup>* mutant expressing His<sub>6</sub>-HoxE (C) were used for pull-down on Co<sup>2+</sup> beads to determine subunit association. Supernatant, flow-through (FT) following bead incubation, pooled washes with/without 0.5 M NaCl, and boiled bead samples from each pull-down were run on TGX Any kDa gradient SDS-polyacrylamide gels (Bio-Rad), transferred to PVDF, and immunoblotted using Hox subunit-specific antibodies.

detectably bound to beads, regardless of whether or not salt was included in the wash (Fig. 5B), validating the presence of a HoxYH subcomplex in soluble extracts. Alternatively, when a His<sub>6</sub>-tagged HoxE is used to pull down the Hox complex, the diaphorase subunits HoxF and HoxU are preferentially associated with the tagged HoxE, whereas only low levels of HoxY and HoxH are present in the bead fraction (Fig. 5C). Interestingly, we observed both processed and unprocessed HoxH associated with HoxY (Fig. 5A) as well as full complex (Fig. 5C). Overall, these data suggest that 1) HoxY and -H bind to each other more strongly than to the diaphorase components, 2) the diaphorase components bind to each other more strongly than to either HoxY or HoxH, and 3) unprocessed HoxH is able to bind HoxY and associate with the full complex.

**Physiological Function of Hox Hydrogenase**—Various phenotypic and activity studies have been reported for *hoxH<sup>-</sup>* (25, 26, 39), *hoxYH<sup>-</sup>* (40), *hoxE<sup>-</sup>* (39), *hoxU<sup>-</sup>* (*Anacystis nidulans*) (14), and *hoxEF<sup>-</sup>* (15, 39) mutants as well as purified complex (19) in cyanobacteria. These studies are difficult to compare because of differences in experimental conditions and/or strain backgrounds. In this study, all of the individual and combined *hox* mutants we created are in the same species and strain background, providing a platform for detailed physiological comparison of hydrogenase activity and growth. Hydrogenase activities of the various *hox* mutants were similar to previously published data (14, 15, 25, 26, 39, 40) (Fig. 6 and supplemental Table 1), confirming that the full complex is necessary for *in vivo* activity and linkage to NAD(P)H and that HoxYH is the minimal hydrogenase with MV as the electron donor. The relative MV-linked activity in diaphorase subunit mutants is consistent with increased levels of unprocessed HoxH (*hoxE<sup>-</sup>*; Fig. 3 and supplemental Fig. 4) or decreased levels of HoxY and HoxH proteins and/or the lack of detectable HoxYH complex

by two-dimensional BN/SDS-PAGE Western blot (*hoxF<sup>-</sup>* and *hoxU<sup>-</sup>*; Figs. 3 and 4).

Previous research on a *hoxH<sup>-</sup>* mutant in *Synechocystis* suggested a slight growth defect when compared with WT cells (25), yet no growth difference was detected in a separate report of a *hoxYH<sup>-</sup>* mutant (40). This inconsistency prompted us to examine WT and *hox<sup>-</sup>* strains of *Synechocystis* under different illumination regimes in an attempt to compare growth under conditions of continuous or quickly cycled (on/off) illumination (Table 1). We hypothesized that quick transitions from darkness to bright illumination may require the Hox hydrogenase to function as an electron valve, a role suggested by previous studies (25, 26), to maintain normal growth rates (25). However, we did not observe a significant difference in doubling times for cultures under either continuous illumination or light/dark cycling conditions with varying durations of dark period (Table 1), consistent with results for similar continuous and light/dark conditions for the *hoxYH<sup>-</sup>* mutant (40). Likewise, we observed no difference in fluorescence-based electron transport rate (ETR) measurements under long term illumination (on a scale of several min) at light intensities between 100 and 1000  $\mu\text{E m}^{-2} \text{s}^{-1}$  for WT versus *hox<sup>-</sup>* cultures (Fig. 7). We further quantified dark-adapted variable fluorescence ( $F_v/F_m$ ) for cells grown under both lower light (65  $\mu\text{E m}^{-2} \text{s}^{-1}$ ) and high light (700  $\mu\text{E m}^{-2} \text{s}^{-1}$ ) and observed no significant difference between WT and *hox<sup>-</sup>* strains under either light regime (Table 2). This is contrary to the findings reported by Antal *et al.* (15), in which light sensitivity and a 20–30% lower  $F_v/F_m$  was measured in a *hoxEF<sup>-</sup>* mutant of *Synechocystis* sp. PCC 6803. In addition, the reported light sensitivity for this *hoxEF<sup>-</sup>* mutation was no longer apparent when transferred to our strain background (supplemental Fig. 5).

## Cyanobacterial Hox Hydrogenase Complex Association and Function

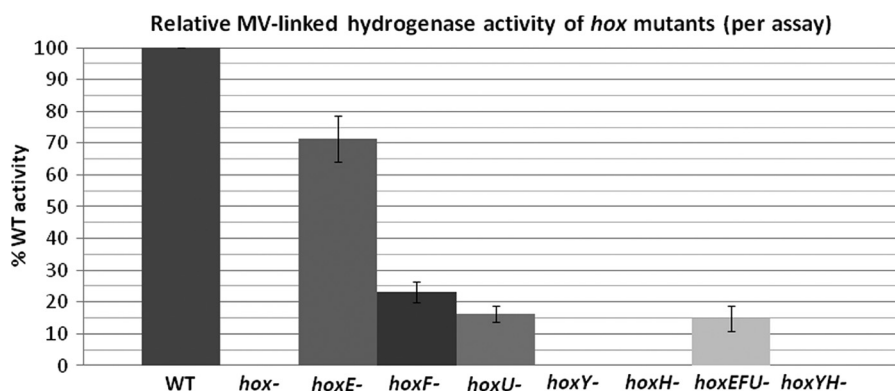


FIGURE 6. **Relative hydrogenase activity of *Synechocystis* sp. PCC 6803 *hox* mutants.** Whole cells of *Synechocystis* sp. PCC 6803 WT and *hox*<sup>-</sup> mutant strains were analyzed for hydrogenase activity with the exogenous electron donor MV. The graph shows MV-linked activities of *hox* mutants relative to WT with assay variation depicted by error bars. Rates (nmol of H<sub>2</sub> ml<sup>-1</sup> min<sup>-1</sup>) are presented in supplemental Table 1.

**TABLE 1**  
Doubling times of WT and *hox*<sup>-</sup> cultures

Growth condition	Doubling time	
	WT	<i>hox</i> <sup>-</sup>
<i>h</i>		
24 h light, 65 μE m <sup>-2</sup> s <sup>-1</sup>		
Aerobic: Bubbled with 2% CO <sub>2</sub> in air	19.5 ± 1.2	21.0 ± 1.2
3 min dark; 3 min light, 1000 μE m <sup>-2</sup> s <sup>-1</sup>		
Aerobic: Bubbled with 2% CO <sub>2</sub> in air	8.9 ± 0.8	10.7 ± 1.3
Microoxic: Bubbled with 2% CO <sub>2</sub> in argon	11.5 ± 1.3	11.7 ± 2.0
15 min dark; 3 min light, 1200 μE m <sup>-2</sup> s <sup>-1</sup>		
Anaerobic: Bubbled with 2% CO <sub>2</sub> in argon	87 ± 8	79 ± 8

## DISCUSSION

Previous studies of the Hox hydrogenase are somewhat variable and fragmented, focused on only one or two subunit mutants (sometimes in different WT strain backgrounds), leaving open questions as to its composition, relative association, and physiological function(s) in *Synechocystis*. Herein, we shed light on these questions by the analysis of Hox subunit mutants, alone or in combination, generated in a common WT strain to ensure that phenotypes observed are solely due to the *hox* mutation and not differences in strain background. Using these strains, we provide comprehensive data on Hox subunit associations, enzyme activities in the absence of individual Hox subunits or subcomplexes, and effects of *hox* mutations on growth and photosynthesis, providing a sound platform to uncover the assembly and physiological role of Hox hydrogenase in future studies.

**Hox Complex/Subcomplex Association in *Synechocystis***—In this work, we present multiple lines of evidence to support the presence of Hox subcomplexes in *Synechocystis*. Our pull-down experiment using a His<sub>6</sub>-tagged HoxE to pull down the full complex resulted in a better recovery of diaphorase proteins (HoxE, HoxF, and HoxU) than hydrogenase proteins (HoxY and HoxH) when comparing protein levels of each subunit on beads versus initial lysate (Fig. 5C). This result is consistent with the 2:1 diaphorase/hydrogenase ratio (with the exception of HoxE; discussed below) of Germer *et al.* (20) when HoxF was tagged for complex purification. Our FPLC and two-dimensional BN/SDS-PAGE analyses of WT soluble extracts (Figs. 1 and 2) uncovered the presence of HoxEFUYH, HoxFUYH, HoxEFU, and HoxFU complexes, but the HoxYH subcomplex was only detectable in the pull-down experiments (Fig. 5). Our

inability to clearly see HoxYH subcomplex association by FPLC and two-dimensional BN methods (Figs. 3B and 4 (B and C)) can possibly be attributed to its instability in the absence of the diaphorase subunits. MV-linked hydrogenase activity measurements of purified His<sub>6</sub>-HoxYH samples decreased considerably during the course of purification (data not shown), consistent with the instability and loss of activity of purified HoxYH subcomplexes in *R. eutropha* (13).

**Hox Complex Purification and Implications for Localization**—Data from FPLC and two-dimensional BN/SDS-PAGE analyses suggest that HoxE may dissociate relatively easily from Hox complexes and subcomplexes, as indicated by the large proportion of this protein present in monomeric form and the presence of HoxFUYH and HoxFU subcomplexes (Figs. 1 and 2). More HoxE protein is detected in lysed whole cell versus soluble protein preparations, and it is the only Hox protein detectable in pellet preparations (data not shown), consistent with the decreased ratio of HoxE (0.2) associated with the purified Hox hydrogenase complex reported by Germer *et al.* (20). Despite the clear localization of this complex in soluble fractions in *R. eutropha* (6), cyanobacterial Hox hydrogenase has been localized, at least in part, to the membrane (42–44), and others have suggested a role for HoxE in anchoring the complex to the membrane in *Synechocystis* (19). We postulate that this membrane association may be required for the association of the complex as a dimer of a pentamer reported by Schmitz *et al.* when purifications were made from an initial 30–50% ammonium sulfate precipitation of whole cell lysates (19). In contrast, Germer *et al.* (20) spun down lysates at high speed prior to a 20% ammonium sulfate addition, centrifugation, and passage of the supernatant through a Streptactin column, whereas we utilized ultracentrifugation of lysates, both of which would probably result in a loss of any complex associated with the membrane (monomer or dimer of Hox complex) and decreased abundance of HoxE. Collectively, these findings suggest that the various subforms of the Hox hydrogenase may become dissociated upon cell breakage and sample preparation or may exist transiently during complex formation, as depicted in our proposed model of assembly (Fig. 8).

**Hox Complex Association and Implications for Maturation and Assembly**—The maturation and assembly of Hox hydrogenase requires six Hyp proteins (HypABCDEF) for biosynthe-

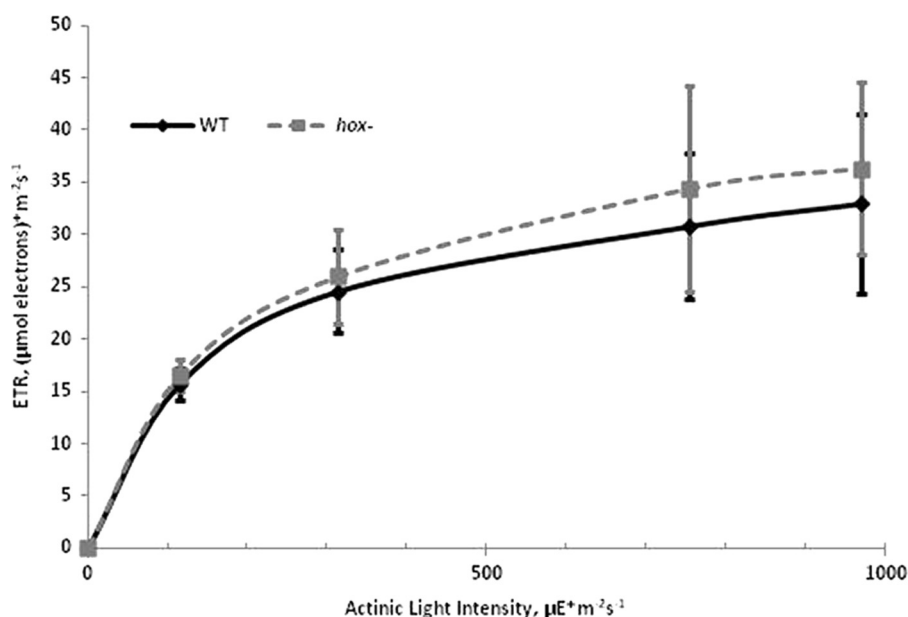


FIGURE 7. Fluorescence-based ETR measurements for *Synechocystis* sp. PCC 6803 WT and  $hox^-$  strains grown under  $50 \mu\text{E m}^{-2} \text{s}^{-1}$  continuous illumination. Variable fluorescence parameters of dilute whole cell suspensions were collected after 3 min of actinic light adaptation at varying intensities.  $\text{ETR} = \Delta F/F_m' \times (\text{actinic light intensity}) \times 0.42$ . Error bars represent standard deviations of three biological replicates.

TABLE 2

Dark-adapted quantum efficiency ( $F_v/F_m$ ) of WT and  $hox^-$  cultures grown under continuous illumination

Illumination during growth	WT	$hox^-$
$\mu\text{E m}^{-2} \text{s}^{-1}$		
65	$0.49 \pm 0.02$	$0.50 \pm 0.02$
700	$0.54 \pm 0.01$	$0.55 \pm 0.01$

sis of the hydrogenase active site (2, 13, 45–48) and an endopeptidase (HoxW) that cleaves the C terminus of HoxH, a step essential for proper folding and final assembly of the active site (49). Unprocessed HoxH band intensities become more pronounced in our  $hoxE^-$  mutant and its complement, a phenomenon that is apparently due to increased transcription and/or translation of the *hox* operon, resulting in increased levels of HoxH (Figs. 3 and 5C and supplemental Figs. 3 and 4; discussed below). Processing of these increased levels of HoxH in the  $hoxE^-$  strain is probably limited by the availability of maturation factors, previously addressed by Germer *et al.* (20) by co-overexpression of the *Synechocystis* *hox* operon using the *psbAII* promoter and ectopic expression of additional maturation factors from *Nostoc* sp. 7120. We were able to detect the co-elution (Fig. 1) and association (Fig. 5) of unprocessed HoxH with other Hox proteins. We were unable to detect this association by two-dimensional BN/SDS-PAGE due to the inability to clearly separate processed and unprocessed HoxH signals and the presence of nonspecific background signals with the  $\alpha$ -HoxH (C-terminal) antibody not apparent in one-dimensional analyses (data not shown). Nevertheless, we were able to detect unprocessed HoxH in the purified HoxYH subcomplex as well as in the full complex using pull-down assays (Fig. 5). The *E. coli* model for [NiFe]-hydrogenase assembly assumes the production of a holo-catalytic subunit prior to its association with the electron-relaying small subunit based on the lack of detection of unprocessed large subunit with the small subunit in purifications (2, 3). In contrast, our results suggest that

HoxY can associate with an unprocessed HoxH prior to its maturation (Fig. 5A). The association of the unprocessed form of HoxH with the full complex is also clearly visible in pull-down experiments (Fig. 5C). We hypothesize that HoxY (and possibly other Hox subunits) may play a role in efficient maturation and processing of HoxH. Alternatively, it is also feasible that HoxH may dimerize, resulting in the association of unprocessed HoxH with full complex or HoxYH subcomplexes already containing processed HoxH (Fig. 8). The events leading to the assembly and maturation of the Hox hydrogenase are largely unknown, and the results here reveal a novel, yet to be identified mechanism of assembly that warrants further studies.

**Hox Subunit Abundance and Complex/Subcomplex Assembly—**Analysis of *hox* deletion strains provides insight into the relative abundance and association of the remaining Hox subunits when other subunits are absent. Various studies have demonstrated that the *hox* operon is transcribed as a single transcript (50–54). Our results confirm expression of all five proteins (Figs. 2 and 3) and suggest a relative balance between the expression of Hox subunits and levels of maturation factors because processing of HoxH and hydrogenase activity are affected negatively by Hox protein overexpression ( $hoxE^-$  or ectopic expression of HoxH; Figs. 3, 5, and 6). Decreased Hox subunit stability is reported in the absence of other hydrogenase subunits in *R. eutropha* (13). In agreement, we observe a decrease in relative abundance of subunits of the hydrogenase (HoxYH) and diaphorase (HoxEFU) subcomplexes in Hox subunit deletion strains, with the exception of HoxE (not present in *R. eutropha*), whose absence actually results in an increase in other Hox protein levels (Fig. 3, A and B; discussed below). Most notably, the relative abundance of remaining Hox subunits (Fig. 3) and resultant hydrogenase activity with MV (Fig. 6) are greatly diminished in strains lacking HoxU. Moreover, despite higher relative protein abundance for remaining Hox subunits in  $hoxE^-$  strains (Fig. 3), detectable subcomplexes are



transcripts (53, 55), which could possibly result from the presence of an antisense RNA just upstream of *hoxU* (56). Because full but not partial deletion of *hoxE* results in increased *hox* transcript levels, there may be some regulatory region in the first 190 nucleotides of *hoxE* that affects transcript stability and/or rate of transcription. In addition, this sequence could also affect rates of translation. Indeed, the online tool RNAfold (57) predicts a decrease in minimal free energy folding for the operon mRNA with *aac3ia* versus *hoxE* when sequences are input and analyzed (supplemental Fig. 3D).

**Synechocystis Hox Hydrogenase Function**—Previous activity measurements of purified Hox complexes and various *hox* mutants in *Synechocystis* and other cyanobacteria demonstrate activity linked to NAD(P)H, *in vivo* and *in vitro*, only with full complex, with the minimal functional hydrogenase, HoxYH, exhibiting activity only in the presence of reduced MV (14, 15, 39, 40). Relative hydrogenase activities of the *hox* mutants we constructed correlate well with calculated relative HoxH (processed) and HoxY protein present in each strain (Figs. 3 and 6 and supplemental Fig. 4). In addition, the substantially decreased MV-linked activity in mutants lacking HoxF and/or HoxU highlights their role in the association of the hydrogenase subcomplex as well as the full complex (Figs. 4 and 6).

In a study by Antal *et al.* (15), the *hoxEF*<sup>−</sup> mutant constructed by Howitt and Vermaas (30) exhibited both light sensitivity and photosynthetic defects when compared with their WT strain, which they interpreted as photosystem II (PSII) photoinhibition due to a lack of hydrogenase activity. We acquired the same *hoxEF*<sup>−</sup> strain and observed similar light sensitivity. However, when we generated the same *hoxEF*<sup>−</sup> mutation in our WT strain background, we no longer observed any light sensitivity when compared with the parental strain (supplemental Fig. 5), suggesting that the defects observed in the published study were not a result of the *hoxEF*<sup>−</sup> mutation. Appel *et al.* (25) also showed a slight growth defect and a difference in PSII/PSI fluorescence kinetics upon illumination under saturating red light in dark-adapted WT and *hoxH*<sup>−</sup> samples. In this study, we compared a *hox*<sup>−</sup> strain derived from the same WT for comparison and observed no defects in growth or light-adapted photosynthesis under many different conditions (Fig. 7 and Table 1), although we did observe a reproducible difference in PSII fluorescence kinetics under saturated red actinic light similar to that reported by Appel *et al.* (25) (data not shown). It is important to note that whereas growth and ETR measurements were taken from time scales on the order of minutes, the PSII fluorescence kinetic measurement happens on the order of seconds. Taken together, our data do not support the hypothesis that the Hox hydrogenase plays a role in photosynthesis or in protection against PSII photoinhibition over extended time scales (on the order of minutes to days). Nevertheless, we cannot exclude the possibility that Hox hydrogenase might play a role as an electron valve during photosynthesis under very transient (on the order of seconds) changes in light intensities that occur in nature. In addition, a lack of phenotype in the *hox*<sup>−</sup> mutant under many different growth regimes (including fermentation; data not shown) rules out a role for the diaphorase as the sole electron donor to the plastoquinone pool in respira-

tion despite homology to missing Complex I components in cyanobacteria, consistent with previous studies (14, 30, 41).

**Conclusions**—This extensive study of the Hox hydrogenase in *Synechocystis* serves to clear up inconsistencies in the literature and reveals new data for subunit and subcomplex interactions that provide a basis for future study of its maturation, assembly, and function. The presence of various complex subforms may represent transient assembly states, suggesting a more complex assembly and maturation scheme than that determined for *E. coli* [NiFe]-hydrogenases. Our data also imply that this assembly may involve association of the unprocessed, immature hydrogenase large subunit with other subunits of the complex prior to full maturation, a previously uncharacterized phenomenon. Analysis of the various Hox subunit and subcomplex mutants in the same strain background confirms previously reported hydrogenase activity results and reveals a correlation between relative levels of HoxY and processed HoxH and activity. A strain containing a deletion of the entire *hox* operon is devoid of any outward phenotypes beyond a lack of hydrogenase activity, demonstrating that its hypothesized role as an electron valve may only be very transient and under specific growth conditions.

**Acknowledgments**—We thank G. Vanzin for construction of *hoxH*<sup>−</sup>; T. Ogawa for WT and *hox*<sup>−</sup> strains; W. Vermaas (Arizona State University) and R. Burnap (Oklahoma State University) for pPETE and pPSBA2KS plasmids, respectively; J. Golbeck (Penn State) for the PsaD antibody; and D. Vinyard (Princeton University) for assistance with PSII fluorescence data interpretation.

## REFERENCES

- Vignais, P. M., and Billoud, B. (2007) Occurrence, classification, and biological function of hydrogenases. An overview. *Chem. Rev.* **107**, 4206–4272
- Forzi, L., and Sawers, R. G. (2007) Maturation of [NiFe]-hydrogenases in *Escherichia coli*. *Biometals* **20**, 565–578
- Magalon, A., and Böck, A. (2000) Dissection of the maturation reactions of the [NiFe] hydrogenase 3 from *Escherichia coli* taking place after nickel incorporation. *FEBS Lett.* **473**, 254–258
- Carriero, D., Wawrousek, K., Eckert, C., Yu, J., and Maness, P. C. (2011) The role of the bidirectional hydrogenase in cyanobacteria. *Bioresour. Technol.* **102**, 8368–8377
- Appel, J. (2012) The physiology and functional genomics of cyanobacterial hydrogenases and approaches towards biohydrogen production. in *Functional Genomics and Evolution of Photosynthetic Systems* (Burnap, R., and Vermaas, W., eds) Illustrated Ed., pp. 357–381, Springer Dordrecht, The Netherlands
- Burgdorf, T., Lenz, O., Buhrke, T., van der Linden, E., Jones, A. K., Albracht, S. P., and Friedrich, B. (2005) [NiFe]-hydrogenases of *Ralstonia eutropha* H16. Modular enzymes for oxygen-tolerant biological hydrogen oxidation. *J. Mol. Microbiol. Biotechnol.* **10**, 181–196
- Schneider, K., Cammack, R., and Schlegel, H. G. (1984) Content and localization of FMN, Fe-S clusters and nickel in the NAD-linked hydrogenase of *Nocardia opaca* 1b. *Eur. J. Biochem.* **142**, 75–84
- Schneider, K., Schlegel, H. G., and Jochim, K. (1984) Effect of nickel on activity and subunit composition of purified hydrogenase from *Nocardia opaca* 1b. *Eur. J. Biochem.* **138**, 533–541
- Maróti, J., Farkas, A., Nagy, I. K., Maróti, G., Kondorosi, E., Rákhely, G., and Kovács, K. L. (2010) A second soluble Hox-type NiFe enzyme completes the hydrogenase set in *Thiocapsa roseopersicina* BBS. *Appl. Environ. Microbiol.* **76**, 5113–5123
- Rákhely, G., Kovács, A. T., Maróti, G., Fodor, B. D., Csanádi, G., Latinov-

- ics, D., and Kovács, K. L. (2004) Cyanobacterial-type, heteropentameric, NAD<sup>+</sup>-reducing NiFe hydrogenase in the purple sulfur photosynthetic bacterium *Thiocapsa roseopersicina*. *Appl. Environ. Microbiol.* **70**, 722–728
11. Rákhely, G., Laurinavichene, T. V., Tsygankov, A. A., and Kovács, K. L. (2007) The role of Hox hydrogenase in the H<sub>2</sub> metabolism of *Thiocapsa roseopersicina*. *Biochim. Biophys. Acta* **1767**, 671–676
  12. Long, M., Liu, J., Chen, Z., Bleijlevens, B., Roseboom, W., and Albracht, S. P. (2007) Characterization of a HoxEFUYH type of [NiFe] hydrogenase from *Allochromatium vinosum* and some EPR and IR properties of the hydrogenase module. *J. Biol. Inorg. Chem.* **12**, 62–78
  13. Massanz, C., Schmidt, S., and Friedrich, B. (1998) Subforms and in vitro reconstitution of the NAD-reducing hydrogenase of *Alcaligenes eutrophus*. *J. Bacteriol.* **180**, 1023–1029
  14. Boison, G., Schmitz, O., Schmitz, B., and Bothe, H. (1998) Unusual gene arrangement of the bidirectional hydrogenase and functional analysis of its diaphorase subunit HoxU in respiration of the unicellular cyanobacterium *Anacystis nidulans*. *Curr. Microbiol.* **36**, 253–258
  15. Antal, T. K., Oliveira, P., and Lindblad, P. (2006) The bidirectional hydrogenase in the cyanobacterium *Synechocystis* sp. strain PCC 6803. *Int. J. Hydrogen Energy* **31**, 1439–1444
  16. Burgdorf, T., van der Linden, E., Bernhard, M., Yin, Q. Y., Back, J. W., Hartog, A. F., Muijsers, A. O., de Koster, C. G., Albracht, S. P., and Friedrich, B. (2005) The soluble NAD<sup>+</sup>-reducing [NiFe]-hydrogenase from *Ralstonia eutropha* H16 consists of six subunits and can be specifically activated by NADPH. *J. Bacteriol.* **187**, 3122–3132
  17. Serebriakova, L. T., and Sheremet'eva, M. E. (2006) Characterization of catalytic properties of hydrogenase isolated from the unicellular cyanobacterium *Gloeocapsa alpicola* CALU 743. *Biochemistry* **71**, 1370–1376
  18. Palágyi-Mészáros, L. S., Maróti, J., Latinovics, D., Balogh, T., Klement, E., Medzihradzky, K. F., Rákhely, G., and Kovács, K. L. (2009) Electron transfer subunits of the NiFe hydrogenases in *Thiocapsa roseopersicina* BBS. *FEBS J.* **276**, 164–174
  19. Schmitz, O., Boison, G., Salzmann, H., Bothe, H., Schütz, K., Wang, S. H., and Happe, T. (2002) HoxE. A subunit specific for the pentameric bidirectional hydrogenase complex (HoxEFUYH) of cyanobacteria. *Biochim. Biophys. Acta* **1554**, 66–74
  20. Germer, F., Zebger, I., Saggi, M., Lendzian, F., Schulz, R., and Appel, J. (2009) Overexpression, isolation, and spectroscopic characterization of the bidirectional [NiFe] hydrogenase from *Synechocystis* sp. PCC 6803. *J. Biol. Chem.* **284**, 36462–36472
  21. McIntosh, C. L., Germer, F., Schulz, R., Appel, J., and Jones, A. K. (2011) The [NiFe]-hydrogenase of the cyanobacterium *Synechocystis* sp. PCC 6803 works bidirectionally with a bias to H<sub>2</sub> production. *J. Am. Chem. Soc.* **133**, 11308–11319
  22. Cournac, L., Guedeney, G., Peltier, G., and Vignais, P. M. (2004) Sustained photoevolution of molecular hydrogen in a mutant of *Synechocystis* sp. strain PCC 6803 deficient in the type I NADPH-dehydrogenase complex. *J. Bacteriol.* **186**, 1737–1746
  23. Cournac, L., Mus, F., Bernard, L., Guedeney, G., Vignais, P., and Peltier, G. (2002) Limiting steps of hydrogen production in *Chlamydomonas reinhardtii* and *Synechocystis* PCC 6803 as analysed by light-induced gas exchange transients. *Int. J. Hydrogen Energy* **27**, 1229–1237
  24. Schütz, K., Happe, T., Troshina, O., Lindblad, P., Leitão, E., Oliveira, P., and Tamagnini, P. (2004) Cyanobacterial H<sub>2</sub> production. A comparative analysis. *Planta* **218**, 350–359
  25. Appel, J., Phunpruch, S., Steinmüller, K., and Schulz, R. (2000) The bidirectional hydrogenase of *Synechocystis* sp. PCC 6803 works as an electron valve during photosynthesis. *Arch. Microbiol.* **173**, 333–338
  26. Gutthann, F., Egert, M., Marques, A., and Appel, J. (2007) Inhibition of respiration and nitrate assimilation enhances photohydrogen evolution under low oxygen concentrations in *Synechocystis* sp. PCC 6803. *Biochim. Biophys. Acta* **1767**, 161–169
  27. Schmitz, O., Boison, G., Hilscher, R., Hundeshagen, B., Zimmer, W., Lottspeich, F., and Bothe, H. (1995) Molecular biological analysis of a bidirectional hydrogenase from cyanobacteria. *Eur. J. Biochem.* **233**, 266–276
  28. Appel, J., and Schulz, R. (1996) Sequence analysis of an operon of a NAD(P)-reducing nickel hydrogenase from the cyanobacterium *Synechocystis* sp. PCC 6803 gives additional evidence for direct coupling of the enzyme to NAD(P)H-dehydrogenase (complex I). *Biochim. Biophys. Acta Protein Struct. M* **1298**, 141–147
  29. Boison, G., Bothe, H., Hansel, A., and Lindblad, P. (1999) Evidence against a common use of the diaphorase subunits by the bidirectional hydrogenase and by the respiratory complex I in cyanobacteria. *FEMS Microbiol. Lett.* **174**, 159–165
  30. Howitt, C. A., and Vermaas, W. F. J. (1999) Subunits of the NAD(P)-reducing nickel-containing hydrogenase do not act as part of the type-1 NAD(P)H-dehydrogenase in the cyanobacterium *Synechocystis* sp. PCC 6803. in *The phototrophic prokaryotes* (Peschek, G. A., Löffelhardt, W., and Schmetterer, G., eds), pp. 595–601, Kluwer Academic/Plenum Publishers, New York
  31. Ikeuchi, M., and Tabata, S. (2001) *Synechocystis* sp. PCC 6803. A useful tool in the study of the genetics of cyanobacteria. *Photosynth. Res.* **70**, 73–83
  32. Kanesaki, Y., Shiwa, Y., Tajima, N., Suzuki, M., Watanabe, S., Sato, N., Ikeuchi, M., and Yoshikawa, H. (2012) Identification of substrain-specific mutations by massively parallel whole-genome resequencing of *Synechocystis* sp. PCC 6803. *DNA Res.* **19**, 67–79
  33. Kuwayama, H., Obara, S., Morio, T., Katoh, M., Urushihara, H., and Tanaka, Y. (2002) PCR-mediated generation of a gene disruption construct without the use of DNA ligase and plasmid vectors. *Nucleic Acids Res.* **30**, E2
  34. Kommalapati, M., Hwang, H. J., Wang, H. L., and Burnap, R. L. (2007) Engineered ectopic expression of the psbA gene encoding the photosystem II D1 protein in *Synechocystis* sp. PCC6803. *Photosynth. Res.* **92**, 315–325
  35. Lagarde, D., Beuf, L., and Vermaas, W. (2000) Increased production of zeaxanthin and other pigments by application of genetic engineering techniques to *Synechocystis* sp. strain PCC 6803. *Appl. Environ. Microbiol.* **66**, 64–72
  36. Boehm, M., Niels, J., Zhang, P., Aro, E. M., Komenda, J., and Nixon, P. J. (2009) Structural and mutational analysis of band 7 proteins in the cyanobacterium *Synechocystis* sp. strain PCC 6803. *J. Bacteriol.* **191**, 6425–6435
  37. Blum, H., Beier, H., and Gross, H. J. (1987) Improved silver staining of plant proteins, RNA and DNA in polyacrylamide gels. *Electrophoresis* **8**, 93–99
  38. Xu, Q., Yu, L., Chitnis, V. P., and Chitnis, P. R. (1994) Function and organization of photosystem I in a cyanobacterial mutant strain that lacks PsaF and PsaJ subunits. *J. Biol. Chem.* **269**, 3205–3211
  39. Aubert-Jousset, E., Cano, M., Guedeney, G., Richaud, P., and Cournac, L. (2011) Role of HoxE subunit in *Synechocystis* PCC6803 hydrogenase. *FEBS J.* **278**, 4035–4043
  40. Pinto, F., van Elburg, K. A., Pacheco, C. C., Lopo, M., Noirel, J., Montagud, A., Urchueguía, J. F., Wright, P. C., and Tamagnini, P. (2012) Construction of a chassis for hydrogen production. Physiological and molecular characterization of a *Synechocystis* sp. PCC 6803 mutant lacking a functional bidirectional hydrogenase. *Microbiology* **158**, 448–464
  41. Schmitz, O., and Bothe, H. (1996) The diaphorase subunit HoxU of the bidirectional hydrogenase as electron transferring protein in cyanobacterial respiration? *Naturwissenschaften* **83**, 525–527
  42. Serebriakova, L., Zorin, N. A., and Lindblad, P. (1994) Reversible hydrogenase in *Anabaena variabilis* ATCC 29413. Presence and localization in non-N<sub>2</sub>-fixing cells. *Arch. Microbiol.* **161**, 140–144
  43. Kentemich, T., Bahnweg, M., Mayer, F., and Bothe, H. (1989) Localization of the reversible hydrogenase in cyanobacteria. *Z. Naturforsch.* **44c**, 384–391
  44. Kentemich, T., Casper, M., and Bothe, H. (1991) The reversible hydrogenase in *Anacystis nidulans* is a component of the cytoplasmic membrane. *Naturwissenschaften* **78**, 559–560
  45. Lutz, S., Jacobi, A., Schlensog, V., Böhm, R., Sawers, G., and Böck, A. (1991) Molecular characterization of an operon (hyp) necessary for the activity of the three hydrogenase isoenzymes in *Escherichia coli*. *Mol. Microbiol.* **5**, 123–135
  46. Hoffmann, D., Gutekunst, K., Klissenbauer, M., Schulz-Friedrich, R., and Appel, J. (2006) Mutagenesis of hydrogenase accessory genes of *Synechocystis* sp. PCC 6803. Additional homologues of hypA and hypB are not

- active in hydrogenase maturation. *FEBS J.* **273**, 4516–4527
47. Casalat, L., and Rousset, M. (2001) Maturation of the [NiFe] hydrogenases. *Trends Microbiol.* **9**, 228–237
  48. Jones, A. K., Lenz, O., Strack, A., Buhrke, T., and Friedrich, B. (2004) NiFe hydrogenase active site biosynthesis. Identification of Hyp protein complexes in *Ralstonia eutropha*. *Biochemistry* **43**, 13467–13477
  49. Wünschiers, R., Batur, M., and Lindblad, P. (2003) Presence and expression of hydrogenase specific C-terminal endopeptidases in cyanobacteria. *BMC Microbiol.* **3**, 8
  50. Gutekunst, K., Phunpruch, S., Schwarz, C., Schuchardt, S., Schulz-Friedrich, R., and Appel, J. (2005) LexA regulates the bidirectional hydrogenase in the cyanobacterium *Synechocystis* sp. PCC 6803 as a transcription activator. *Mol. Microbiol.* **58**, 810–823
  51. Oliveira, P., and Lindblad, P. (2005) LexA, a transcription regulator binding in the promoter region of the bidirectional hydrogenase in the cyanobacterium *Synechocystis* sp. PCC 6803. *FEMS Microbiol. Lett.* **251**, 59–66
  52. Oliveira, P., and Lindblad, P. (2008) An AbrB-Like protein regulates the expression of the bidirectional hydrogenase in *Synechocystis* sp. strain PCC 6803. *J. Bacteriol.* **190**, 1011–1019
  53. Kiss, E., Kós, P. B., and Vass, I. (2009) Transcriptional regulation of the bidirectional hydrogenase in the cyanobacterium *Synechocystis* 6803. *J. Biotechnol.* **142**, 31–37
  54. Oliveira, P., and Lindblad, P. (2009) Transcriptional regulation of the cyanobacterial bidirectional Hox-hydrogenase. *Dalton Trans.* 9990–9996
  55. Dutheil, J., Saenkham, P., Sakr, S., Leplat, C., Ortega-Ramos, M., Bottin, H., Cournac, L., Cassier-Chauvat, C., and Chauvat, F. (2012) The AbrB2 autorepressor, expressed from an atypical promoter, represses the hydrogenase operon to regulate hydrogen production in *Synechocystis* strain PCC6803. *J. Bacteriol.* **194**, 5423–5433
  56. Mitschke, J., Georg, J., Scholz, I., Sharma, C. M., Dienst, D., Bantscheff, J., Voss, B., Steglich, C., Wilde, A., Vogel, J., and Hess, W. R. (2011) An experimentally anchored map of transcriptional start sites in the model cyanobacterium *Synechocystis* sp. PCC6803. *Proc. Natl. Acad. Sci. U.S.A.* **108**, 2124–2129
  57. Gruber, A. R., Lorenz, R., Bernhart, S. H., Neuböck, R., and Hofacker, I. L. (2008) The Vienna RNA Websuite. *Nucleic Acids Res.* **36**, W70–W74